



# International Journal of Sciences: Basic and Applied Research (IJSBAR)

ISSN 2307-4531  
(Print & Online)

<http://gssrr.org/index.php?journal=JournalOfBasicAndApplied>



---

## Kinetic and Thermodynamic Study of Triton X-100 Removal from Aqueous Solution of Functionalized Mesoporous Silica

Sameer H. Kareem<sup>a</sup>, Inaam H. Ali<sup>b\*</sup>, Moayyed Q. Jalhoom<sup>c</sup>

<sup>a,b</sup> Chemistry Department, College of Science for Women, Baghdad University, Iraq

<sup>c</sup> Ibn-Sina State Company, Ministry of Industrial and Minerals, Baghdad, Iraq

<sup>b</sup> Email: [inaam.mohammed@yahoo.com](mailto:inaam.mohammed@yahoo.com)

### Abstract

In this work, batch adsorption experiments were carried out for the removal of Triton X-100 as a pollutant surfactant from aqueous solutions on mesoporous silica as adsorbents. These silica functionalized with organic groups (methyl and amine) were produced from two different silica precursor (sodium silicate and tetraethoxysilane) using sol-gel method. The effects of major variables governing the efficiency of the process such as dosage of mesoporous silica (25-125 mg), temperature (288-318 K), and initial surfactant concentration (15-120 mg/l), were investigated. Equilibrium data were fitted to the Langmuir, Freundlich and Dubinin-Radushkevich (D-R) isotherm models and isotherm constants were determined. The equilibrium data were best represented by the Langmuir isotherm model. The adsorption kinetic data were analyzed using pseudo-first-order, pseudo-second-order and intra particles diffusion models. It was found that the pseudo-second order kinetic model was the most appropriate model, describing the adsorption kinetics and the intra-particle diffusion is not the only rate limiting mechanism and that some other mechanisms also play an important role. Thermodynamic parameters such as changes in the free energy of adsorption ( $\Delta G^\circ$ ), enthalpy ( $\Delta H^\circ$ ) and entropy ( $\Delta S^\circ$ ) were calculated.

---

\* Corresponding author.

E-mail address: [inaam.mohammed@yahoo.com](mailto:inaam.mohammed@yahoo.com).

The negative values of ( $\Delta G^\circ$ ) indicate that the surfactant adsorption process is spontaneous in nature and the positive value of ( $\Delta H^\circ$ ) shows the endothermic nature of the process.

**Keywords:** Triton X-100; Methylfunctionalized mesoporous silica; Aminofunctionalized mesoporous silica; Adsorption.

## 1. Introduction

Surfactants are widely used in many industrial and commercial products and processes, such as soaps and detergents, industrial processes requiring colloid stability, metal treatments, mineral flotation, pesticides, oil production, pharmaceutical formulation, emulsion polymerization, and particle growth [1].

Some processes have been employed in order to solve the environmental problems caused by surfactants, including adsorption, anaerobic and aerobic degradation, and biodegradation. One of the common methods to remove surfactants from water is to use adsorption technology. Surfactant adsorption has been studied extensively through using several materials as surfactant adsorbents. These include activated carbons [2], zeolites [3], silica [4], mineral oxides (alumina) [5], polymers [6].

The adsorption of nonionic surfactants at solid surfaces is of interest because of its importance to a great number of industrial and technological processes associated with colloidal stability and detergency. Most nonionic surfactants contain polar groups that form hydrogen bonds with the hydroxyl groups on the solid surface [7].

Triton X-100 ( $C_{14}H_{22}O(C_2H_4O)_n$ ) (Figure 1) is a nonionic surfactant which has a hydrophilic polyethylene oxide chain (on average it has 9.5 ethylene oxide units) and an aromatic hydrocarbon lipophilic or hydrophobic group. The hydrocarbon group is a 4-(1,1,3,3-tetramethylbutyl)-phenyl group.

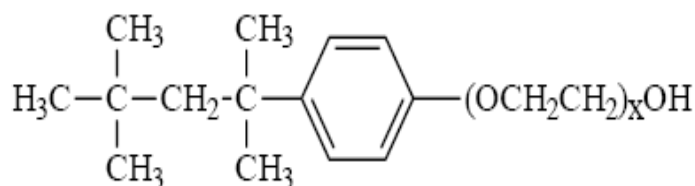


**Figure 1:** Chemical Structure of Triton X-100

The adsorption of TX-100 on a carbon paste electrode was investigated by voltammetry [8]. The results showed that TX-100 exhibited two types of adsorptive behavior at a carbon paste electrode at different concentration ranges. Yusuf et al. [9] studied of aqueous  $CO_2$  foam prepared by a mixtures hydrophilic silica nanoparticles and non-ionic Triton X-100. They found that the adsorption behavior of TX-100 on silica surface exhibit a particular characteristics depend on the concentration of silica, high total surface area available leads to high adsorption of surfactant molecules. MCM-41(Mobile Crystalline Material) was used to adsorb nonionic surfactant Triton X-114 [10]. FTIR and NMR methods were used to study the interaction between the surfactant and the adsorbent.

Mesoporous materials, such as mesoporous silica with diameters of 2 to 50 nm, show high promise to be used as adsorbents for such organic materials because of their high porosity and their large surface areas. Functionalization of the surface of these mesoporous materials with organic or inorganic functional groups leads to new physical and chemical properties. The specific porous structure and the excellent textural properties of mesoporous silica allow easier diffusion of large molecules into the active sites [11].

This study aim to remove the surfactant Triton X-100 from aqueous solution on mesoporous silica produced from two types of silica precursor and they are functionalized with methyl and amino organic groups. These are: MMPS-SS (methyl functionalized mesoporous silica produced from sodium silicate), MMPS-TEOS (methyl functionalized mesoporous silica produced from tetraethoxy silicate), AMPS-SS (amino functionalized mesoporous silica produced from sodium silicate), and AMPS-TEOS (amino functionalized mesoporous silica produced from tetraethoxy silicate).

## 2. Materials and Methods

### 2.1. Materials

**Adsorbents:** Methyl and amino functionalized mesoporous silica were prepared using one-step synthesis method which based on hydrolysis and condensation of silica precursor [sodium silicate or tetraethyl orthosilicate (TEOS)] with different organosilane [methyltriethoxysilane (MTES) and aminopropyltriethoxysilane (APTES)] using the silicone surfactant polydimethylsiloxane- polyethylene oxide (PDMS-PEO) as template[12,13]. Table (1) Show textural properties of these prepared adsorbents determined by nitrogen adsorption at 77 K using volumetric surface analyzer (Micromeritics).

**Table 1:** Textural Properties of Adsorbents

Adsorbents	Surface area (m <sup>2</sup> /g)	Pore volume (cm <sup>3</sup> /g)	Pore size (nm)
MMPS-SS	43.4	0.1782	16.39
MMPS-TEOS	646.9	0.0118	14.49
AMPS-SS	3.27	0.4202	2.762
AMPS- TEOS	19.96	0.0749	13.68

**Adsorbate:** Triton X-100 has an average of 9.5 ethylene oxide units per molecule was purchased from BDH chemicals Ltd.

### 2.2. Adsorption Experimental

Batch experiments were conducted by contacting different amounts (25, 50, 75, 100 and 125) mg of functionalized MPS adsorbents (MMPS-SS, MMPS-TEOS, AMPS-SS and AMPS-TEOS) with 50 ml of surfactant TX-100 solution having concentration range (15-120 mg/L). The temperature was fixed at 298K and the agitation speed of thermostatic shaker bath was kept at 200 rpm for all experiments. These samples were

shaken well for enough time to reach equilibrium. The particles of functionalized MPS were separated from the mixture by centrifugation at 3000 rpm. The concentrations of the surfactant solutions before and after the adsorption were determined by UV-Visible spectrophotometer at  $\lambda_{\max}$  223. The experiments were repeated at least twice. The amount of surfactant adsorbed was determined by the equation:

$$q_e = \frac{(C_o - C_e)V}{w} \dots \dots (1)$$

Where  $C_o$  is the initial concentration (mg/L),  $C_e$  is the equilibrium concentration (mg/L),  $V$  is the volume of the solution (L) and  $w$  is the amount of MPS (g).

The effect of temperature on the removal of TX-100 was studied using four temperatures in the range of 288-318 K using the thermostatic shaker bath.

The kinetic study of TX-100 adsorption was performed by mixing the amount of adsorbents with 50 ml of TX-100 (60 mg/L) aqueous solution in 250 mL flasks immersed in the thermostatic shaker bath in the temperature range (288-318) K. At various time intervals, the concentration of solution was determined by measuring absorbance at maximum characteristic wavelength 223 nm.

### 3. Results and Discussion

#### 3.1. The Effect of Adsorbent Dose of MPS on Adsorption of TX-100

The influence of adsorbent amount on TX-100 removal by functionalized MPS with methyl and amine groups are shown in Figure (2). The results indicated that at constant concentration of TX-100 (120mg/l) and variation the adsorbent dosage of functionalized MPS from 25mg/50ml to 125mg/50ml at 298K, the removal percentage of TX-100 was reached maximum value about 91% using 50 mg of MMPS-TEOS, 85% using 75mg of MMPS-SS, 78% using 100mg of AMPS-TEOS and 75% using 100mg of AMPS-SS. This behavior may be due to as the dosage of adsorbent increased, the adsorption sites remain unsaturated during the adsorption reaction leading to drop in adsorption capacity or due to aggregation/agglomeration of sorbent particles at higher concentrations, which would lead to a decrease in the surface area and an increase in the diffusional path length [14]. These doses were fixed through other experiments.

#### 3.2. The Effect of Contact Time and initial concentration on Adsorption of TX-100.

The effect of contact time on the adsorption of TX-100 on functionalized MPS is illustrated in Figures (3) and (4). High pore diffusion of surfactant molecules into the bulk of adsorbents were observed in the case of using functionalized of MPS with methyl group which show speed uptake and reached contact time after 30 min. While it needed 60 min when using MPS functionalized with amino groups. The rapid uptake at the initial contact time can be attributed to the availability of the positively charged surface of aminofunctionalized MPS. The slow rate of TX-100 adsorption is probably due to the slow pore diffusion of the solute molecules into the bulk of the adsorbent [15].

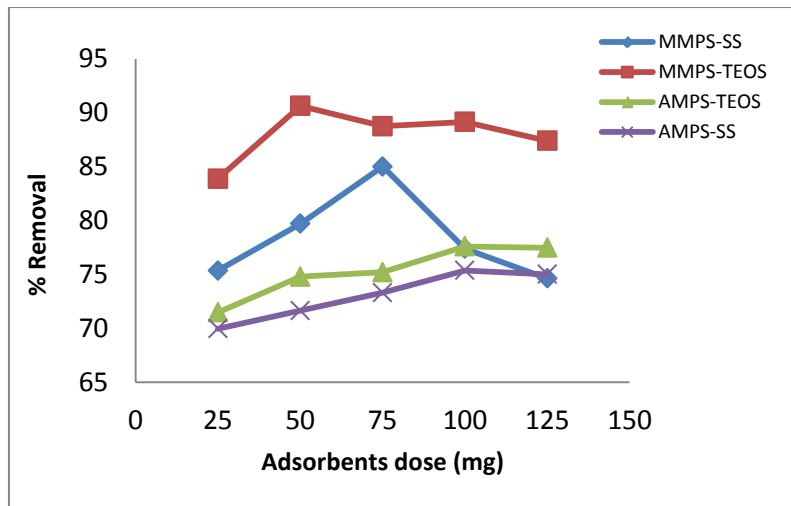


**Figure 2:** The effect of Adsorbent dosage of MPS on removal of TX-100 at initial concentration 120mg/l and at 298 K temperature.

Figures (3) and (4) show that surfactant removal was highly dependent on initial surfactant concentration. The larger removal amount of TX-100 caused by a higher initial TX-100 concentration was presumably attributed to the active interaction between adsorbents and surfactant molecules. The findings probably were also due to an increase in surfactant concentration could accelerate the diffusion of TX-100 molecules to the adsorbents as a result of an increase in the driving force of concentration gradient. With the progress of adsorption, the availability of adsorption sites of the adsorbents got diminished, leading the adsorption capacity to be constant [16].

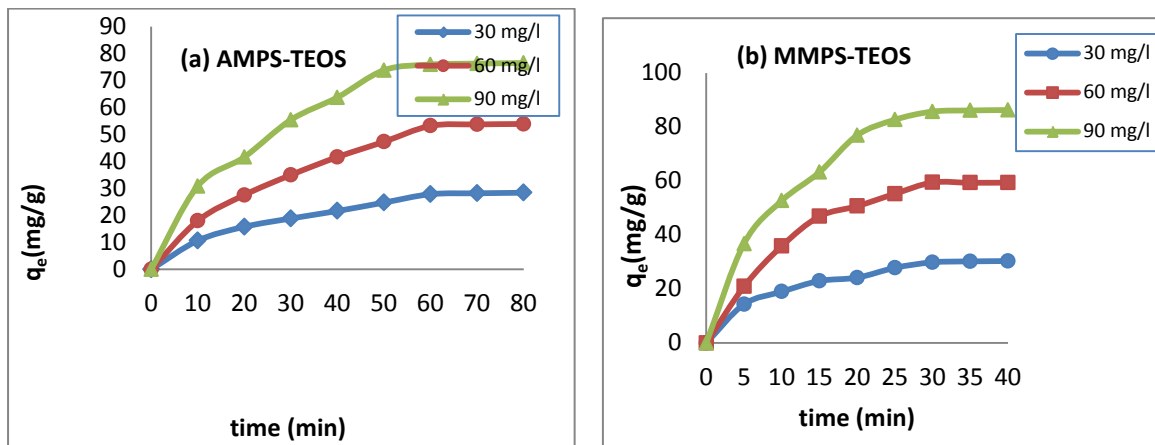
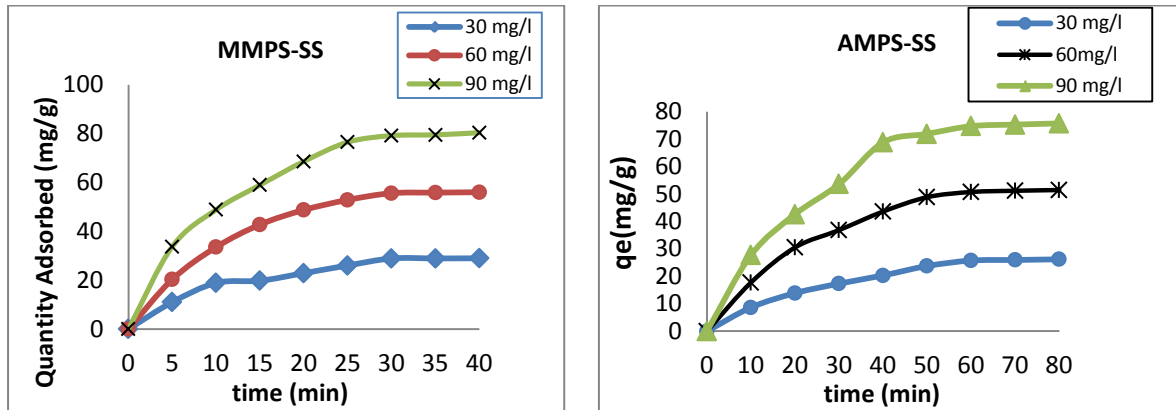


**Figure 3:** The effect of initial concentration and contact time on removal of TX-100 using 50, 75 mg of (a): AMPS-TEOS, (b): MMPS-TEOS.

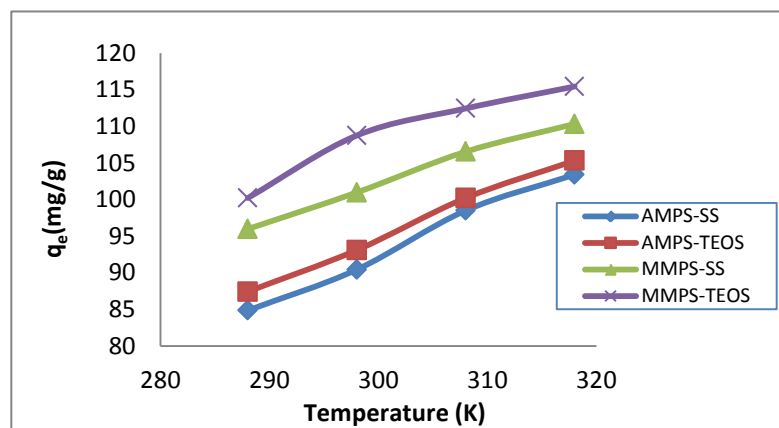
### 3.3. The Effect of temperature on adsorption of TX-100

Figure (5) shows the effect of temperature (288-318) K on the removal of TX-100 (120mg/l) on the methylfunctionalized MPS and aminofunctionalized MPS. It showed that an increase in temperature, adsorption

of TX-100 will increase which indicates the process is endothermic and the sorption is mainly absorption. When the temperature increased from 288 to 318 K the maximum amount adsorbed increased from 84.8 to 103.4 mg/g, 87.4 to 105.3 mg/g, 95.9 to 110.3 mg/g and 100.23 to 115.5 mg/g using AMPS-SS, AMPS-TEOS, MMPS-SS and MMPS-TEOS as adsorbent respectively. This may be interpreted as, increase in temperature increases collision frequency and also high temperature may be raise either dimensions of porous or activation energy [17].



**Figure 4:** The effect of initial concentration and contact time on removal of TX-100 using 100 mg of (a): MMPS-SS, (b): AMPS-SS.



**Figure 5:** The effect of temperature on adsorption of TX-100 on functionalized MPS.

### 3.4. Adsorption Isotherm of TX-100 on functionalized MPS

Adsorption isotherm of TX-100 on functionalized MPS at 298 K was illustrated in Figure (6). The study showed that the adsorption isotherm of TX-100 on functionalized MPS was nonlinear and typical S-shape curves, except the isotherm on MMPS-TEOS which shows L-shape curve.

Langmuir, Freundlich and Dubinin-Radushkevich (D-R) models were chosen to describe the relationship

between the amounts of TX-100 adsorbed on functionalized MPS and its equilibrium concentration at four different temperatures.

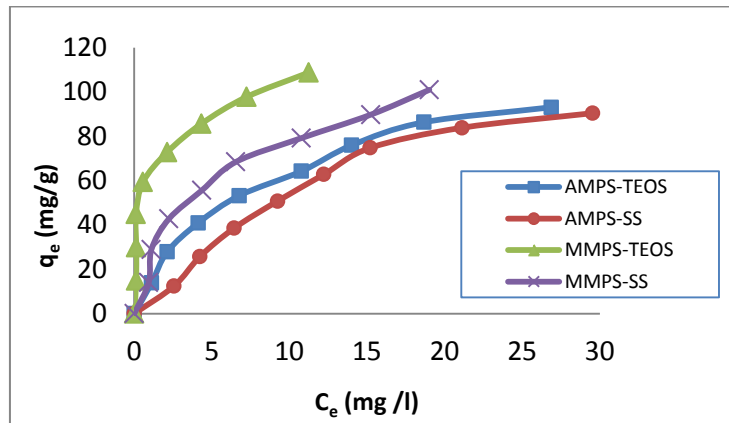


Figure 6: Adsorption isotherm of TX-100 on functionalized MPS at 298 K.

For solid-liquid interaction the linear form of Langmuir isotherm [18]:

$$\frac{C_e}{q_e} = \frac{1}{K_L \cdot Q^\circ} + \frac{C_e}{Q^\circ} \dots \dots \dots (2)$$

Where C<sub>e</sub> is the concentration of dye at equilibrium, q<sub>e</sub> is the amount of dye adsorbed at equilibrium, Q<sup>°</sup> (mg/g) and K<sub>L</sub> (L/mg) are the Langmuir constants. Q<sup>°</sup> is the monolayer adsorption capacity and K<sub>L</sub> is the constant related to the free energy of adsorption. The Langmuir constants Q<sup>°</sup> and K<sub>L</sub> were determined from the slope and intercept respectively when C<sub>e</sub>/q<sub>e</sub> was plotted against C<sub>e</sub>.

The Freundlich model is given in its linear form as Equation (3) [19]:

$$\ln q_e = \ln K_f + \frac{1}{n} \ln C_e \dots \dots \dots (3)$$

where, K<sub>f</sub> is the Freundlich constant related to overall adsorption capacity (mg/g); and 1/n is a dimensionless constant related to the intensity of adsorption, or the heterogeneity factor describes reversible adsorption and is not restricted to the formation of the monolayer. Values of K<sub>f</sub> and n respectively are obtained from intercept and slope of the linear plot of lnq<sub>e</sub> versus ln C<sub>e</sub>.

Dubinin-Radushkevich isotherm is another isotherm equation that applied in this study. For solid-liquid interaction the linear form of Dubinin–Radushkevich (D–R) isotherm (equation 4) can be written as follows [20]:

$$\ln q_e = \ln q_m - \beta \varepsilon^2 \dots \dots \dots (4)$$

Where  $\varepsilon$  is the Polanyi potential which equal:

$$\varepsilon = RT \ln \left( 1 + \frac{1}{c_0} \right) \dots \dots \dots (5)$$

$q_m$  is the adsorption capacity of the adsorbent ( $\text{mg g}^{-1}$ ),  $\beta$  is a constant related to the adsorption energy ( $\text{mol}^2 \text{kJ}^{-2}$ ),  $R$  is the gas constant ( $\text{JK}^{-1} \text{mol}^{-1}$ ), and  $T$  is the temperature (K). The D-R model is important for predicting the nature of adsorption process through the determination of the mean adsorption energy ( $E$ ) using equation [21]:  $E = \frac{1}{\sqrt{2\beta}}$

The linear plots of the three equations for the adsorption of TX-100 surfactant on the four MPS adsorbents at 298K are shown in Figs (7-9). The correlation coefficient  $R^2$  value of each plot was used to describe the applicability of the isotherm models. The different isotherm parameters obtained from the slope and intercept of the plots with their correlation coefficient values are presented in Table (2).

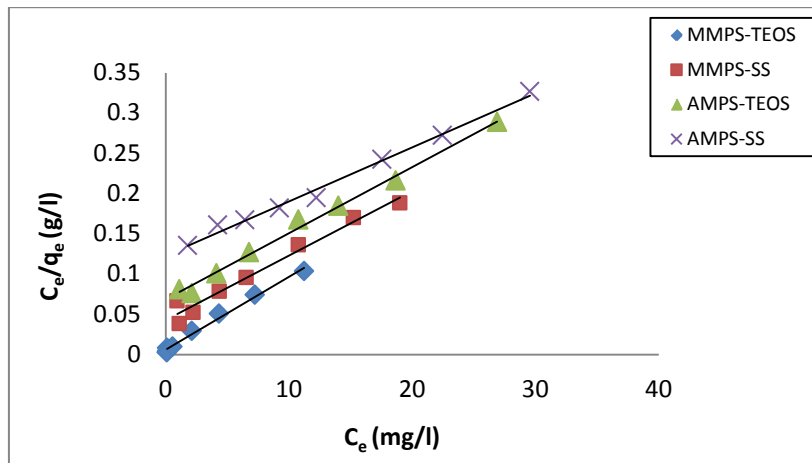


**Figure 7:** Linear plot of Langmuir models for adsorption of TX-100 on functionalized MPS at (298)K.

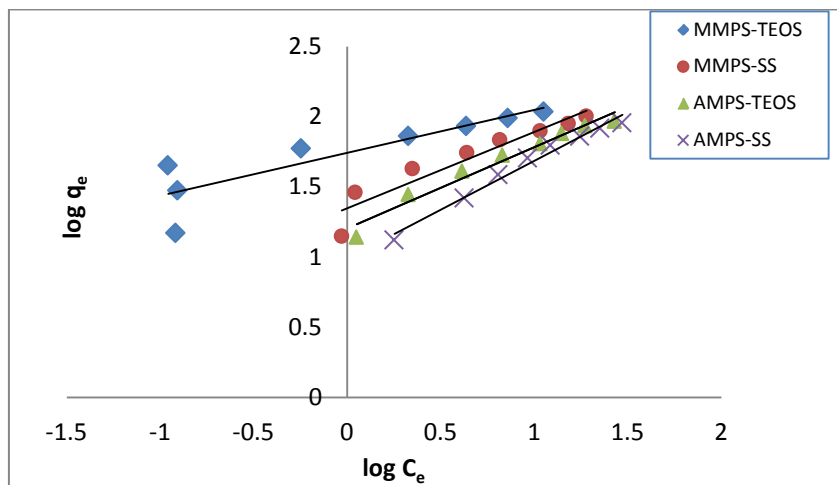


**Figure 8:** Freundlich models for adsorption of TX-100 on functionalized MPS at (298)K.



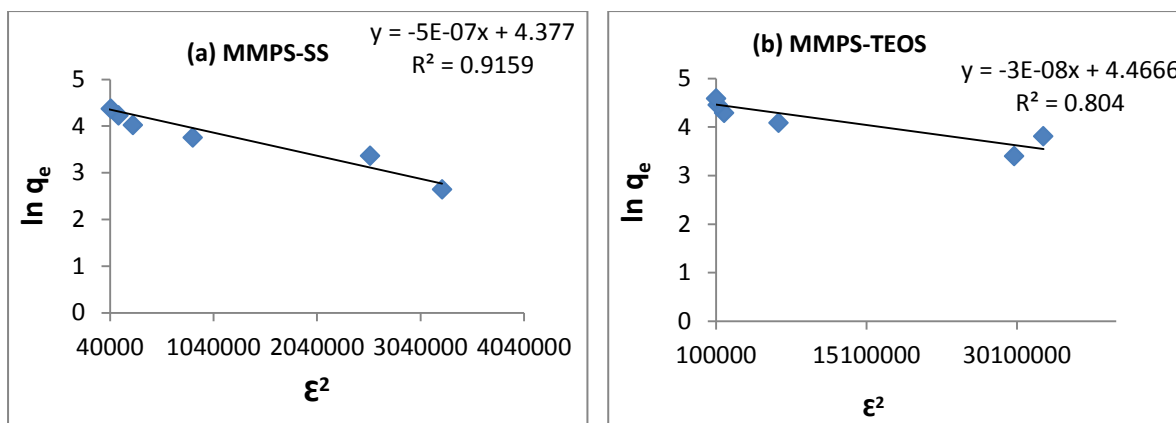


**Figure 9:** Typical linear plots of Dubinin-Radushkevich of adsorption of TX-100 on (a) MMPS-SS, (b) MMPS-TEOS at 298K.

**Table 2:** The values of parameters and correlation coefficient of Langmuir, Freundlich and Dubinin-Radushkevich equations.

Models		Langmuir			Freundlich			Dubinin-Radushkevich		
Type of MPS	Temp. (K)	Q <sup>0</sup> (mg/g)	K <sub>L</sub> (L/g)	R <sup>2</sup>	K <sub>f</sub>	n	R <sup>2</sup>	q <sub>m</sub> (mg/g)	E (kJ mol <sup>-1</sup> )	R <sup>2</sup>
AMPS-SS	288	142	0.049	98.4	14.09	1.92	98.9	64.65	0.353	87.1
	298	142	0.052	99.5	10.35	1.47	98.3	78.73	0.353	91.3
	308	166	0.076	90.3	13.30	1.38	92.8	79.12	0.707	93.4
	318	142	0.266	99.4	28.18	1.81	94.5	79.12	1.581	89.4
MMPS-SS	288	200	0.0370	95.5	8.77	1.30	99.3	64.78	0.500	77.1
	298	125	0.1904	97.0	22.2	1.84	96.0	79.59	1.000	91.5
	308	142	0.250	96.5	28.1	1.75	89.6	85.71	1.290	91.9
	318	125	0.888	99.2	47.31	2.26	87.1	88.05	3.779	88.3
AMPS-TEOS	288	142	0.050	97.2	9.35	1.50	97.4	64.07	0.500	86.3
	298	125	0.117	99.3	16.0	1.73	96.4	68.92	0.845	86.8
	308	142	0.179	99.2	22.4	1.76	95.0	73.62	1.290	85.6
	318	125	0.421	99.5	33.8	1.95	92.8	78.02	2.236	86.1
MMPS-TEOS	288	166	0.085	97.0	12.3	1.34	98.6	71.09	0.707	82.6
	298	111	1.60	98.9	55.2	3.27	77.2	87.00	4.082	80.4
	308	125	1.80	98.7	60.4	2.94	77.5	88.49	5.000	80.0
	318	125	4	99.6	83.9	2.71	83.6	104.5	5.000	93.0

It can be seen from the correlation coefficient values that the Langmuir isotherm (Fig 7) model fitted the data best followed by the Freundlich model, while the values obtained for the Freundlich constant  $n$  ( $1 < n < 10$ ) is an indication that functionalized MPS has a high affinity for TX-100 molecules. The mean adsorption energy  $E$  calculated from D-R model (Fig 9) reveals that the adsorption of TX-100 onto functionalized MPS was dominated physical adsorption since all values of  $E$  are less than  $8\text{kJmol}^{-1}$ [22].

### 3.5. The kinetic study

Three of the most widely used kinetic models, Lagergren-first-order equation, pseudo-second-order equation and intraparticle diffusion equation have been used to research the adsorption kinetic behavior of MB(10 mg/l) onto MPS at (288-318) K. The best fit model was selected based on the linear regression correlation coefficient values ( $R^2$ ).

The equations of these kinetic models are given in the following:

a) The linear form of the pseudo-first order kinetic model of [23] can be expressed as follows:

$$\log(q_e - q_t) = \log q_e - (k_1/2.303) t \dots\dots\dots (6)$$

where  $k_1$  is the rate constant of the pseudo-first order kinetics ( $\text{min}^{-1}$ ).  $q_e$  and  $q_t$  are the amounts adsorbed on the surface of the adsorbent at equilibrium and at any time ( $\text{mg g}^{-1}$ ) respectively. The  $q_e$  and  $k_1$  are calculated from the intercept and the slope of plots of  $\log (q_e - q_t)$  vs  $t$ , respectively.

b) The linear form of the pseudo-second order kinetic model [24] is given as follows:

$$\frac{t}{q_t} = \frac{1}{k_2 q_e^2} + \left(\frac{1}{q_e}\right) t \dots\dots\dots (7)$$

where  $k_2$  is the rate constant of the pseudo-second order kinetics ( $\text{g mg}^{-1} \text{min}^{-1}$ ).  $k_2$  and  $q_2$  are calculated from the intercept and the slope of plots of  $t/q_t$  against  $t$ , respectively.

c) The equation of the intra-particle diffusion model of Weber and Morris [25] can be expressed as follow:

$$q_e = k_d t^{1/2} + C \dots\dots\dots (8)$$

where,  $k_d$  is intra-particle diffusion rate constant ( $\text{mg g}^{-1} \text{min}^{-1/2}$ ), and  $C$  is intercept. This model reflects that pore diffusion occurs due to the porous nature of adsorbent. The rate constant of the intra-particle diffusion ( $k_d$ ) can be estimated from the slope of the linear portion of the plot of the amount of solute adsorbed ( $q_e$ ) against square root of time ( $t^{1/2}$ ).

The results obtained for the three models are depicted in Figures (10-12) and the best fitted model determined depending on the linear correlation coefficient  $R^2$ . The results obtained from the slope and intercept of the plots are shown in Table (3).

The correlation coefficient of pseudo second-order (Figure 11) which close to unit was much higher than that of pseudo first-order (Figure 10) although the theoretical  $q_e$  values computed from pseudo second –order and pseudo first-order did not give reasonable values with experimental  $q_e$  values.

From Table (3), it can be seen that the pseudo-second order kinetic rate constants increased with the increasing

of temperature for all adsorbents. This is due to the fact that temperature increases the collision of particles and consequently the adsorption rate will become faster [26]. Also the initial rate of reaction (h) at 298K can be arranged as follow:

$$\text{MMPS-TEOS} > \text{MMPS-SS} > \text{AMPS-SS} > \text{AMPS-TEOS}$$

We noticed that the rate of reaction increased as increasing in surface area of adsorbents except AMPS-SS is higher reaction rate that from AMPS-TEOS although it has smaller surface area. This can be explained as the pore size of AMPS-SS larger than that of AMPS-TEOS.

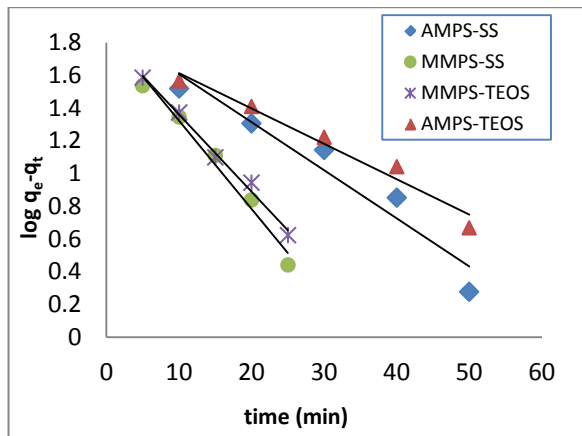


**Figure 10:** Pseudo first order plot of kinetics adsorption of TX-100 (60mg/l) on functionalized MPS at 298K.

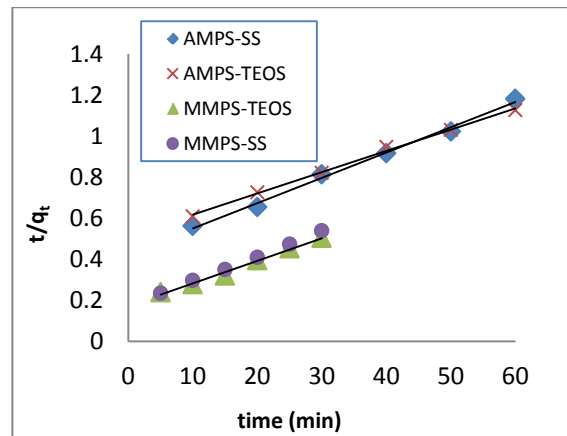


**Figure 11:** Pseudo second order plot of kinetics adsorption of TX-100 (60mg/l) on functionalized MPS at 298K.

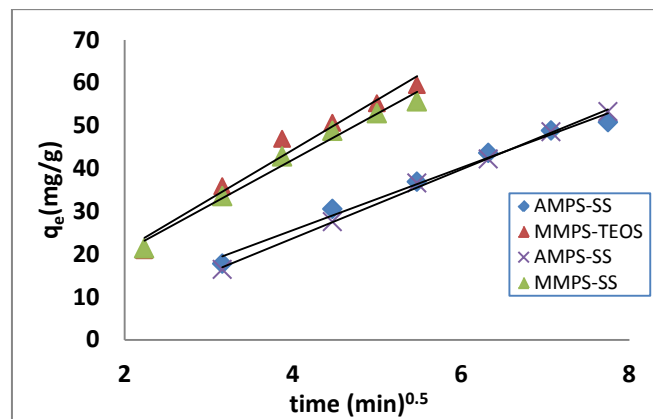


**Figure 12:** Intraparticles diffusion kinetics for adsorption of TX-100 onto functionalized MPS.

The  $R^2$  value of diffusion model was high which indicate that the adsorption of TX-100 on functionalized MPS can be followed by intra-particle diffusion model. However, the lines do not pass through the origin as shown in Figure (12), indicating that the intra-particle diffusion is not the only rate limiting mechanism and that some

other mechanisms also play an important role [27]. Surface adsorption and interparticle diffusion were likely to take place simultaneously; both processes control the kinetics of surfactant-MPS adsorbent interaction.

**Table (3):** Kinetic parameters for adsorption of TX-100 on functionalized MPS at different temperatures.

Type of MPS	Models		Pseudo first order				Pseudo second order				Diffusion model	
	Temp (K)	q <sub>e</sub> (exp.) mg/g	q <sub>e</sub> mg/g	k <sub>1</sub> min <sup>-1</sup>	R <sup>2</sup>	q <sub>e</sub> mg/g	k <sub>2</sub> mg/g min	h= qe <sup>2</sup> k <sub>2</sub>	R <sup>2</sup>	k <sub>d</sub> mg/g min <sup>-0.5</sup>	R <sup>2</sup>	
AMPS-SS	288	47.50	61.65	0.0575	96.4	76.92	0.000375	2.218	99.8	6.653	98.7	
	298	50.76	79.43	0.0667	93.1	83.33	0.000336	2.333	99.4	7.287	97.2	
	308	54.44	67.92	0.0552	96.6	100	0.00037	3.700	99.5	7.529	98.7	
	318	57.34	63.53	0.0598	95.3	76.92	0.00066	3.904	99.5	6.726	97.4	
MMPS-SS	288	50.22	87.49	0.1496	95.8	83.33	0.000676	4.694	98.8	10.39	96.9	
	298	55.64	72.77	0.1220	97.9	83.33	0.000832	5.777	99.8	10.73	98.1	
	308	57.46	85.11	0.1451	93.0	90.90	0.00077	6.362	99.7	10.86	97.8	
	318	59.00	86.49	0.1612	96.8	76.92	0.00152	8.993	99.7	9.762	95.2	
AMPS-TEOS	288	49.33	81.65	0.0598	90.5	111.1	0.00013	1.604	98.5	7.933	99.4	
	298	53.22	67.60	0.0483	96.6	100	0.00019	1.900	99.7	8.039	99.8	
	308	56.64	71.28	0.0506	95.6	100	0.00023	2.300	99.4	8.261	99.7	
	318	58.43	74.13	0.0644	91.8	83.3	0.000474	3.289	99.2	7.436	99.4	
MMPS-TEOS	288	53.56	116.4	0.0170	90.1	90.90	0.000593	4.899	98.7	11.21	97.2	
	298	59.43	67.60	0.0108	99.1	90.90	0.000703	5.808	99.0	11.64	96.8	
	308	59.78	88.92	0.1381	98.0	100	0.00062	6.200	98.7	12.00	96.8	
	318	59.98	112.7	0.1681	95.2	90.90	0.000812	6.709	99.1	11.61	96.1	

**3.6. Thermodynamic study of adsorption of TX-100 on functionalized MPS**

Adsorption experiments were conducted at 288, 298, 308 and 318 K to study the thermodynamic (equilibrium) parameters (free energy change ( $\Delta G^\circ$ ), enthalpy change ( $\Delta H^\circ$ ), and entropy change ( $\Delta S^\circ$ ) associated with the adsorption of Tx-100 on the functionalized MPS samples. The Langmuir isotherm was used to calculate thermodynamic parameters using the following linear form equations [28, 29]:

$$\Delta G^\circ = -RT \ln K_L \dots \dots \dots (9)$$

$$\ln K_L = \frac{\Delta S^\circ}{R} - \frac{\Delta H^\circ}{RT} \dots \dots \dots (10)$$

where  $K_L$  is the Langmuir equilibrium constant (l/mol); R is the gas constant (8.314 J/mol K) and T is the temperature (K). Considering the relationship between ( $\Delta G^\circ$ ) and  $K_L$ , ( $\Delta H^\circ$ ) and ( $\Delta S^\circ$ ) were determined from the slope and intercept of the van't Hoff plots of  $\ln(K_L)$  versus  $1/T$ . The results were illustrated in Table (4) and the relation between Langmuir constant and temperature was in Figure (13). The negative values of  $\Delta G^\circ$  at all

temperatures indicate the spontaneous nature of TX-100 adsorption on functionalized MPS. The values of  $\Delta G^\circ$  for adsorption of TX-100 on AMPS-SS was from -8.2036 to -13.515, on MMPS-SS was from -7.5168 to -16.706, on AMPS-TEOS was from -8.252 to -14.7428, and on MMPS-TEOS was from -9.5084 to -19.252  $\text{KJmol}^{-1}$  during the temperature change from 288 to 318K. So, according to the previous results, the adsorption of Tx-100 on functionalized MPS was predominantly physical adsorption. The positive values of  $\Delta H^\circ$  for adsorption of TX-100 revealed that the process is an endothermic process. This phenomenon may be due to the behavior of TX-100 in aqueous solution, which displaced more than single water molecule adsorbed previously on functionalized MPS which leads to endothermic adsorption process [30].

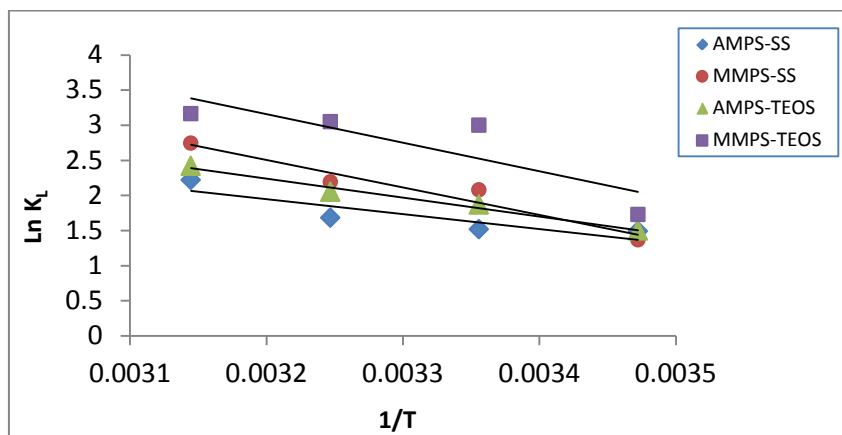


Figure 13: Plot of  $\ln K_L$  versus  $1/T$  for estimation of thermodynamic parameters.

Table 4: Thermodynamic parameters of adsorption of TX-100 on functionalized MPS.

Type of MPS	Temp.(K)	$\Delta G^\circ$ (kJ/mol)	$\Delta H^\circ$ (kJ/mol)	$\Delta S^\circ$ (J/K.mol)
AMPS-SS	288	-8.2036	17.7	72.8
	298	-8.6509		
	308	-9.9129		
	318	-13.515		
AMPS-TEOS	288	-7.5168	22.4	90.4
	298	-11.836		
	308	-12.931		
	318	-16.704		
MMPS-SS	288	-8.2520	32.5	124.7
	298	-10.642		
	308	-12.081		
	318	-14.7428		
MMPS-TEOS	288	-9.5084	33.8	134.4
	298	-17.110		
	308	-17.986		
	318	-19.252		

In addition the small values of  $\Delta H^\circ$  ( $17.7 - 33.8 \text{ KJ.mol}^{-1}$ ) are not compatible with the formation of strong chemical bonds between TX-100 molecules and the sites on functionalized MPS surface.  $\Delta S^\circ$  is positive since the displaced water molecules gain more translational entropy than is lost by the TX-100 leading to increase randomness at the solid/solution interface [31].

#### **4. Conclusions**

The study of adsorption TX-100 on methyl and amino functionalized mesoporous silica indicate the following:-

- The adsorption is monolayer coverage adsorption process due to comply of the adsorption isotherm with the Langmuir equation.
- The adsorption on functionalized MPS with methyl group gave high adsorption capacity due to the high surface area, however, low adsorption capacities were observed by amino functionalized mesoporous silica which might be ascribed to the blockage of pores with these large molecules.
- The adsorption is physisorption, this is reflected by the values of  $\Delta H^\circ$  and E obtained from Vants Hoff and Dubinin-Radushkovich equations.
- Kinetics investigation have reflected that pseudo-second order kinetics equation is found as the best model for fitting kinetics data and intraparticle diffusion model is necessary through rate determining step reaction
- Thermodynamic data results obtained has indicated that the adsorption processes are spontaneous and endothermic in nature.

#### **References**

- [1] P. C .Pavan, E. L. Crepaldi and . J. B. Valim, "Sorption of anionic surfactants on layered double hydroxides" *J. Colloid Interface Sci.* 229:346-352, 2000.
- [2] W. Zhou Zhu "Enhanced soil flushing of phenanthrene by anionic-nonionic mixed Surfactant" *J. water Research.*,42:101-108, 2008.
- [3] R. A.Garcia-Delgado , L. M. Cotoruelo, and J. J. Rodriguez. "Adsorption of Anionic Surfactant Mixtures by Polymeric Resins". *Sep. Technol.* 27 :1065-107,1992.
- [4] J. J. Kipling. *Adsorption from Solutions of Non- Electrolytes.* London Academic Press,. 1965
- [5] A. K. Vanjara, and S. G. Dixit, "Formation of mixed aggregates at the alumina. Aqueous surfactant solution interface". *Langmuir*, 11(7), 2504, 1995.
- [6] W. Brown, and J. Zhao, "Adsorption of sodium dodecyl sulfate on polystyrene latex particles using dynamic light scattering and zeta potential measurements". *Macromolecules*, 26: 2711-2715, (1993).
- [7] R. Zhang,; and P. Somasundaran, "Advances in adsorption of surfactants and their mixtures at solid/solution interfaces". *Advances in Colloid and Interface Science*, 123-126, 2006.
- [8] A. W. David. "Dynamics of Surfactant Adsorption at Solid-Liquid Interfaces" Ph.D. Thesis, University of Durham, 2011, p8.
- [9] S. Yusuf,; M. Muhammad, and Z. J. Mohd. "Aqueous Foams Stabilized by Hydrophilic Silica Nanoparticles via In-Situ Physisorption of Nonionic TX-100 Surfactant". *Iranica Journal of Energy & Environment.* 4(1): 8-16, 2013.

- [10] T. Paulina, "FTIR And NMR Studies Of Adsorbed Triton X-114 In MCM-41 Materials" *Indo. J. Chem.* 9 (2):184-188, 2009.
- [11] M. M. Branda, R. A. Montani, and N. J. Castellani. "The Distribution of Silanols on the Amorphous Silica Surface: A Monte Carlo Simulation" *Surf. Sci.*, 446, L89, 2000.
- [12] S. H. Kareem, I. H. Ali, M. Q. Jalhoom, "Synthesis and Characterization of Organic Functionalized Mesoporous Silica and Evaluate their Behavior for Removal of Methylene Blue from Aqueous Solution" *American Journal of Environmental Science*, 10(1); 48-60, 2014.
- [13] S. H. Kareem, I. H. Ali, M. Q. Jalhoom, "Synthesis, Characterization and Textural Analysis of functionalized Mesoporous Silica Using Sodium Silicate as Precursor and Silicone Surfactant as Template" *Journal of Baghdad for Science*, 2014,
- [14] P. Santanu, and C. K. Kartic, A review on experimental studies of surfactant adsorption at the hydrophilic solid-water interface. *Advanced in Colloidal and Interfaces Science*, 110(3):75-95, 2004.
- [15] S. M. Yakout and A. A. Nayl, "Removal of cationic surfactant (CTAB) from aqueous solution on to activated carbon obtained from corncob". *Carbon-Sci. Tech.* 2:107-116, 2009.
- [16] R. Zhang, and P. Somasundaran, "Advances in Adsorption of Surfactant and their Mixtures at Solid/Solution interfaces". *Adv. Colloid Interface Sci.*, 123-126:213-229, 2006.
- [17] N. Barbara, B. Christine, and J. Jean-Luc, "The dynamic surface tension of atmospheric aerosol surfactants reveals new aspects of cloud activation. *Nature Communications*, 5:1-7, 2014.
- [18] Langmuir, (1918) The Adsorption of Gases on Plane Surfaces of Glass, Mica and Platinum, *J. Amer. Chem. Soc.* 40(9):1316-1403.
- [19] H.M.F. Freundlich. "Over the adsorption in solution". *J. Phys. Chem.*, 57: 385-470, 1906.
- [20] M.M Dubinin. "The potential theory of adsorption of gases and vapors for adsorbents with energetically non-uniform surface". *Chem. Rev.* 60:235-266, 1960.
- [21] A. Cleiton, E. Nunes, C. Mário, and Guerreiro. "Estimation of Surface Area And Pore Volume of Activated Carbons by Methylene Blue and Iodine Numbers". *Quim. Nova.* 34(3): 472-476, 2011.
- [22] I. H. Shireen, "Adsorption of Triton X-100 Surfactant on Different Agricultural Soils" *National Journal of Chemistry*, 35:415-426, 2009.
- [23] S. Lagergren, "For the theory so-called adsorption of dissolved substances. *Kungliga Svenska Vetenskapsakademiens Handlingar*, 24(4):1-39, 1898.
- [24] G. McKay, and Y.S. Ho. "Pseudo-second order model for sorption processes. *Process*". *Biochem.* 34: 451-465, 1999.
- [25] W.L. Weber, and J.C. Morris, "Kinetics of adsorption on carbon from solution". *J. San. Eng. Div. ASCE*, 89:31-39, 1963.
- [26] R. B. Nihar, and P. Santanu, "Effect of Electrolyte Solutions on the Adsorption of Surfactants at PTFE-Water". *Ind. Eng. Chem. Res.* 49:7060-7067, 2010.
- [27] J. Abdul Salam, and N. Das, "Biosorptive Removal of Lindane Using Pretreated Dried Yeast-Equilibrium and Kinetic Studies". *International Journal of Pharmacy and Pharmaceutical Sciences*, 5(3): 987-993, 2013.
- [28] Y. Onal, "Kinetics of adsorption of dyes from aqueous solution using activated carbon prepared from waste apricot". *J. Hazard. Mater.* 137: 1719-1728, 2006.

- [29] C. Pinghuo, Z. Xuezhen,; L. Yongxiu,; and L. Dongping,. “Kinetics and Thermodynamic Study adsorbing Methelene Blue on Nanozirconia” *Applied Mechanics and Materials*, 5:1311-1319, 2014.
- [30] Z. Rui, P. Somasundaran. “Advances in adsorption of surfactants and their mixtures at solid/solution interfaces” *Advances in Colloid and Interface Science* 123-126:213-229, 2006.
- [31] R. B. Nihar, “Studies on Adsorption and Wetting Phenomena Associated with Solid Surfaces in Aqueous Synthetic and Natural Surfactant Solutions”. Ph.D thesis, National Institute of Technology, (2012). p141.